Food Research International 157 (2022) 111241

Contents lists available at ScienceDirect

Food Research International

journal homepage: www.elsevier.com/locate/foodres

Integrated metabolomics and transcriptomics reveal the adaptive responses of *Salmonella enterica* serovar Typhimurium to thyme and cinnamon oils

Lin Chen [a,b], Xue Zhao [a,b], Rui Li [c], Hongshun Yang [a,b,*]

[a] Department of Food Science and Technology, National University of Singapore, Singapore 117542, Singapore
[b] National University of Singapore (Suzhou) Research Institute, 377 Lin Quan Street, Suzhou Industrial Park, Suzhou, Jiangsu 215123, PR China
[c] School of Horticulture, Hainan University, Haikou, Hainan 570228, PR China

ARTICLE INFO

Keywords:
Essential oil
Foodborne pathogen
Resistance development
Metabolomics
Transcriptomics
Foodomics
Food safety
Antimicrobial agent

ABSTRACT

Essential oils (EOs), such as thyme (Thy) and cinnamon (Cin) oils, present promising antibacterial properties against foodborne pathogens (e.g., *Salmonella enterica* serovar Typhimurium). However, the food matrix might result in sublethal EO stress, and little information about direct and/or cross-resistance development after sublethal EO exposure is available. This study revealed that *S.* Typhimurium under sublethal Thy and Cin (50% minimum inhibitory concentration, MIC_{50}) treatments exhibited a lower growth rate and an extended lag phase. EO adapted cells showed direct-resistance to subsequent lethal EO treatment, and cross-resistance to thermal (58 °C) and oxidative (hydrogen peroxide, 50 mmol/L) stresses. Metabolomics analysis revealed changes of 47 significant metabolites (variable importance in projection > 1, false discovery rate (FDR) < 0.05), including lipids, oligopeptides, amino acids, nucleotide related compounds, and organic acids. Metabolic pathways, such as aminoacyl-tRNA biosynthesis, were shown to be involved in EO adaptation. Furthermore, a transcriptomics study identified 161 differentially expressed genes (DEGs, fold change > 2, FDR < 0.05) in MIC_{50} Thy treated cells, while more DEGs (324) were screened from the MIC_{50} Cin group. The integrated omics analysis allowed us to speculate on the molecular mechanisms. Under harsher Thy stress, *S.* Typhimurium cells adopted a conservative strategy to survive. By contrast, more radical responses were observed during Cin adaptation. In conclusion, the food industry should be more cautious in the use of EOs because sublethal EO stress might result in the development of resistance.

1. Introduction

Foodborne pathogens, such as *Escherichia coli*, *Salmonella enterica*, and *Listeria monocytogenes*, cause around 600 million illnesses and 420,000 deaths worldwide annually (Chen et al., 2020). *S. enterica* are Gram-negative, facultatively anaerobic, flagellated rod-shaped bacteria with a low infectious dose. *Salmonella*-caused salmonellosis is characterized by acute enterocolitis, accompanied by inflammatory diarrhea. The control of pathogenic *S. enterica* in foods is difficult because of their high adaptive abilities and complex food environments. Moreover, food products can be contaminated by *S. enterica* at each point in the food supply chain, including processing, distribution, preparation, and consumption (Jarvis et al., 2016).

Food safety scientists are constantly searching for effective natural antimicrobials, because of consumers' increasing demand for safe and nutritive foods (Yuan et al., 2018). Plant-derived essential oils (EOs) have been used historically in food (as flavorings), cosmetics, traditional medicine, and aromatherapy. In the food safety field, EOs have attracted intensive interest in recent decades because of their antioxidant activities, wide-spectrum antimicrobial properties, and generally recognized as safe (GRAS) status. For instance, thyme (Thy) and cinnamon (Cin) EOs have exhibited promising antimicrobial activities against *S. enterica* serovar Typhimurium, *E. coli*, and *L. monocytogenes* in different food matrices (Hyldgaard et al., 2012). Boskovic et al. (2017) reported that the counts of a *Salmonella* cocktail were reduced by 1.69–4.05 log CFU/g in minced pork meat after Thy treatment. Moreover, >5.0 log CFU/g reductions of *Salmonella* spp. and *L. monocytogenes* in cantaloupe melons under Cin nanoemulsion treatment were observed by Paudel et al. (2019). Therefore, EOs, such as Thy and Cin, could be a promising strategy to control *S. enterica*.

Bacteria have evolved various adaptive strategies to cope with different environmental stresses. For example, the abuse of antibiotics

* Corresponding author at: Department of Food Science and Technology, National University of Singapore, Singapore 117542, Singapore.
E-mail address: fstynghs@nus.edu.sg (H. Yang).

https://doi.org/10.1016/j.foodres.2022.111241
Received 22 December 2021; Received in revised form 5 April 2022; Accepted 7 April 2022
Available online 16 April 2022

has led to the emergence of multi-drug resistant *S. enterica*, which has become a significant public health problem. Furthermore, hydrophobic EO components tend to interact with components of the food matrix (e.g., fat, starch, and proteins) in many food products. The antibacterial effects of EOs are reduced by food ingredients, resulting in a sublethal EO environment for pathogens (Hyldgaard et al., 2012; Yuan et al., 2018). Previous studies have revealed that sublethal stresses, such as mild heat or acid, can induce adaptive responses in pathogens, thus making them more resistant to subsequent lethal treatments (da Silva et al., 2015; Wesche et al., 2009). Therefore, the frequent use of sublethal levels of EOs might induce stress adaptation, resulting in EO-resistant bacteria. A report showed that *E. coli* exhibited increased direct and cross-resistance after 10-days' consecutive adaptation to carvacrol and citral (Chueca et al., 2016). To the best of knowledge, little information about EO resistance development in *S.* Typhimurium is available.

Emerging omics techniques, such as metabolomics, proteomics, and transcriptomics, provide a feasible method to obtain global physicochemical profiles of microorganisms. For example, the transcriptomic responses of *S. enterica* to oxidative stress revealed by Wang et al. (2010) helped develop more effective hurdle interventions. Transcriptomics is a high-throughput application that can quantify the transcriptome in cells. It provides quantitative and qualitative information regarding gene expression differences. Proteomics is often applied as a complementary technique to study the expression, regulation, and function of the whole set of proteins (Tan et al., 2009). Compared with proteomics, metabolomics provides distinct advantages: It is more closely related to the phenotype, such as tolerance, making it a powerful tool to study the molecular mechanisms in response to stresses (Tan et al., 2009; Teoh et al., 2015). Thus, the integrated transcriptomics and metabolomics analyses of sublethal EO–treated *S. enterica* might provide valuable information about the adaptive mechanisms.

We hypothesized that *S. enterica*, under sublethal EO stress, might develop EO resistance, and multiple molecular mechanisms would contribute to the adaptation process. Thus, the present study aimed to evaluate adaptation to EOs (Thy and Cin) and the underlying adaptive mechanisms. The minimum inhibitory concentrations (MICs) of selected EOs against *S.* Typhimurium were tested, and the induced resistances of bacteria cultured in sublethal EOs were further evaluated. Moreover, ultra-high performance liquid chromatography quadrupole time-of-flight mass spectrometry (UPLC-QTOF-MS) and RNA sequencing (RNA-seq) were applied to study the metabolomic and transcriptomic profiles of *S.* Typhimurium during resistance development.

2. Materials and methods

2.1. Bacterial culture conditions

A frozen stock of *S.* Typhimurium (ATCC 14028) was purchased from the American Type Culture Collection (ATCC, Manassas, VA, USA) and stored at −80 °C. The strain resuscitation was conducted by inoculating the stock into 10 mL of tryptone soya broth (TSB, Oxoid, Basingstoke, UK) and incubating at 37 °C overnight. Daily transfer was conducted to keep cell viability. A working suspension of *S.* Typhimurium was prepared by inoculating the overnight cultures into 20 mL of TSB (1:100, v/v) and then incubating at 37 °C for approximately 10 h. The bacterial concentration was examined by plate culture on tryptone soya agar (TSA, Oxoid). Cells at the early stationary phase were centrifuged at 4500*g* for 10 min at 24 °C, and then washed with phosphate-buffered saline (PBS, 0.1 mol/L, pH 7.2) twice. The obtained cell pellets were resuspended and diluted to the appropriate concentrations in TSB (Chen et al., 2019).

2.2. MIC determination

Food grade EOs, including Thy (W306509), Cin (W229105), garlic (W250309), ginger (W252204), and fennel (W248207) oils, were purchased from Sigma-Aldrich (St. Louis, MO, USA). EO stock solutions (400 mg/mL) were prepared in analytical grade ethanol (Sigma-Aldrich) and stored at 4 °C in the dark before use. The Clinical and Laboratory Standards Institute microdilution method was applied to determine the MICs of the EOs (Yuan et al., 2018). Briefly, EOs were continuously 2-fold diluted in TSB in a 96-well plate (Thermo Fisher Scientific, Waltham, MA, USA). An equal volume (100 μL) of prepared EO and bacterial solutions were mixed. The final EO concentration range was 10.0 to 0.02 mg/mL and the microbial inoculum level was 10^5 CFU/mL. After incubation at 37 °C for 24 h, 10 μL of resazurin (0.01%, w/v) was added into each well and the mixtures were further incubated for 2 h (37 °C) before examining the color change. The minimum EO concentration required to inhibit microbial growth was defined as the MIC. TSB with highest ethanol concentration (2.5%, v/v) was determined to have no effect on microbial survival (data not shown). TSB inoculated with *S.* Typhimurium and TSB without inoculation were used as positive and negative controls, respectively.

2.3. Gas chromatography–mass spectrometry analysis of selected EOs

The EOs showing antibacterial effects on *S.* Typhimurium were analyzed on a 7890A gas chromatography (GC)-7200 MS system (Agilent Corp., Santa Clara, CA, USA). The selected EOs (50 mg) were dissolved in ethanol (10 mL) and mixed well. After filtering through a 0.45 μm filter membrane, the samples were injected into the GC equipped with an HP-5MS column (30 m × 0.25 mm, 0.25 μm). The flow rate of the carrier gas (highly pure He) was 1.0 mL/min. The injector temperature was 250 °C, and the split mode was applied (1:50). The column temperature was increased from 100 to 200 °C at 4 °C/min, and then held for 5.0 min. The MS conditions were set as follow: Mass range, 30–450 amu; 70 eV electron energy and scan mode electron impact; 250 °C ion source temperature (Guo et al., 2021). The major compounds in the EO samples were identified by comparing the obtained 70 eV mass spectra with those in the Nist90 and Wiley5 libraries. The GC peak areas were used to calculate the relative contents of the identified components.

2.4. Growth kinetics of S. Typhimurium in sublethal EOs

Overnight cultured *S.* Typhimurium was inoculated into 10 mL of TSB containing the selected EO at one-half MICs (MIC_{50}). The cells were cultured at 37 °C, and the growth kinetics were determined by sampling at appropriate time intervals, diluting in peptone water (Oxoid), and plating on TSA. The cell counts (log CFU/mL) were plotted against culture duration, and the obtained growth curves were fitted using the Baranyi and Roberts model (Zhao et al., 2020). Three independent biological replicates were prepared, and each biological replicate represented three technical replicates.

2.5. Direct and cross-resistances examination

EO adapted and non-adapted cells at the early stationary phase were inoculated (final inoculum, 10^5 CFU/mL) into TSB containing Thy or Cin at the MIC. The mixtures were sampled at appropriate time intervals, diluted in peptone water, and plated on TSA. Survival curves were plotted and regressed using a linear model. D values (min) were calculated to compare the induced direct-resistance (Yuan et al., 2018).

Heat resistance was tested by inoculating *S.* Typhimurium cells into 10 mL of pre–warmed TSB at 58 °C in a water bath. Aliquots were withdrawn and cooled in iced water immediately for 10 min before plating.

Oxidative stress resistance was determined by inoculating *S.* Typhimurium cells into 10 mL of PBS containing 50 mmol/L hydrogen peroxide (H_2O_2, Sigma-Aldrich) at room temperature.

Acid resistance (AR) was tested using simulated gastric fluid (SGF),

which comprised the following components: 8.3 g/L proteose-peptone (Oxoid), 3.5 g/L D-glucose (Sigma–Aldrich), 2.05 g/L NaCl (Sigma-Aldrich), 0.6 g/L KH_2PO_4 (Sigma-Aldrich), 0.11 g/L $CaCl_2$ (Sigma-–Aldrich), 0.37 g/L KCl (Sigma-Aldrich), 0.1 g/L lysozyme (Sigma-–Aldrich), and 13.3 g/L pepsin (Sigma-Aldrich). The final pH of the SGF was adjusted to 1.5 using 5.0 mol/L HCl (Sigma-Aldrich). The microbial resistance test was conducted in a water bath at 37 °C, and survival counts were determined by periodically sampling and plating. Three independent biological replicates were prepared, and each biological replicate represented three independent technical replicates.

2.6. Metabolomics analysis

UPLC-QTOF-MS-based metabolomics analysis was conducted to determine the metabolic differences between the adapted *S.* Typhimurium cells and the non-adapted control. Cells in each group were collected at the early stationary phase by centrifugation (4500*g*, 10 min, 24 °C). The obtained bacterial pellets were immediately mixed with ice–cold methanol (Sigma-Aldrich), and frozen in liquid nitrogen. The mixtures were thawed on ice and then frozen in liquid nitrogen to destroy the cell membrane. The freeze–thaw cycles were performed three times, and the mixtures were stored at −20 °C overnight for extraction. Intracellular metabolites were obtained by centrifugation at 12,000*g* for 20 min (4 °C). Three biological replicates without technical replicates in each group were prepared. Samples were stored at −80 °C before use (Zhao et al., 2020a,b).

The extracts were separated using an Agilent Technologies 1290 Infinity UPLC system (Agilent Corp.), equipped with an Acquity UPLC HSS T3 column (2.1 × 100 mm, 1.8 μm; Waters, Singapore). The column oven was maintained at 25 °C, and the auto–sampler was kept at 4 °C. The flow rate was 0.3 mL/min, and the injection volume was 2 μL. The mobile phase, consisting of 0.1% formic acid in water (A) and 0.1% formic acid in acetonitrile (B), was applied for gradient elution using the following program: 1% B, 0–1.5 min; 1–99% B, 1.5–18 min; 99% B, 18–21 min; 99–1% B, 21–21.1 min; and 1% B, 21.1–26 min (Yu et al., 2019). Mass spectrometry of the separated metabolites was performed using an Agilent 6540 UHD Accurate-Mass Q-TOF mass spectrometer (Agilent Technologies), equipped with an electrospray ionization (ESI) interface. The *m/z* range was set at 50–1000 with a scan rate of 2 spectra/s. Nitrogen at 320 °C was used for desolvation at a flow rate of 10 L/min. Other parameters were capillary voltage, 3500 V; skimmer, 45 V; and nebulizer, 35 psi. Targeted MS/MS was conducted using collision energies (0, 10, 20, and 40 V). The scan *m/z* range was 100–850, with a scan rate of 3.30 spectra/s. MS/MS data were acquired with an isolation width of ~ 4 amu.

The obtained UPLC-MS raw data were converted to the mzXML format, and then uploaded to the MassIVE database (https://massive.ucsd.edu/ProteoSAFe/static/massive.jsp) with accession number MSV000088070. The mzXML files were further imported into XCMS (https://xcmsonline.scripps.edu/) for non-linear alignment, time domain, filtering, and extraction of the peak intensities. Principal component analysis (PCA) was applied to discriminate groups with different metabolic profiles (Vong et al., 2018). The intensity profiles were further input into SIMCA software (version 13.0, Umetrics, Umeå, Sweden) to conduct pairwise orthogonal partial least squares discriminant analysis (OPLS-DA). The most significant features were screened using variable importance in projection (VIP) analysis. Features with a VIP > 1 and a false discovery rate (FDR) < 0.05 were identified using Metlin (https://metlin.scripps.edu/), the Human Metabolome Database (https://hmdb.ca/), the PubChem Database (https://pubchem.ncbi.nlm.nih.gov/), and the MS/MS spectra. Enrichment and pathway analyses were conducted using MetaboAnalyst 5.0 (https://www.metaboanalyst.ca/) (Liu et al., 2020).

2.7. Transcriptomics analysis

RNA-seq was applied to study the transcriptional responses of *S.* Typhimurium under sublethal EO stresses. Cultures of *S.* Typhimurium at the early stationary phase in each group were stabilized using RNAprotect Bacteria reagent (Qiagen, Hilden, Germany). Thereafter, total RNA was extracted from the cells using an RNA Mini-Pre Kit (Bio Basic, Ontario, Canada) with on-column DNase digestion. A spectrophotometer (BioDrop, Biochrom, Cambridge, UK) was used to test the quality and concentration of the RNA in the samples. Moreover, the RNA integrity was checked using 1% (w/v) agarose gel electrophoresis. Pure RNA samples without contamination were further enriched using oligo (dT) beads. The RNA Integrity Number (RIN) was analyzed using an Agilent 2100 Bioanalyzer system (Agilent Corp.). Furthermore, rRNA was removed from the total RNA (RIN > 8.5) using a Ribo-Zero bacterial rRNA removal kit (Illumina, San Diego, CA, USA). The obtained mRNA was fragmented randomly by adding fragmentation buffer, and cDNA was synthesized according to the manufacturer's instructions (Illumina). The final cDNA libraries were constructed by PCR using the purified cDNA fragments. The qualified libraries were sequenced in an Illumina sequencers (HiSeq 4000, Illumina) using the paired-end technology with a read length of 2 × 150 bp. Three biological replicates without technical replicates in each group were prepared (Chin et al., 2017).

The RNA-seq raw data were processed using the statistical software R (version 4.0.4). The qualities of the reads before and after quality and adaptor trimming were assessed using the FastQC package. Illumina adaptors and low quality reads were removed using the Trimmomatic program. The trimmed reads were then aligned to the reference genome (*S.* Typhimurium str. LT2, NC_003197) using HISAT2. Potential transcripts were assembled and quantified by the StringTie package. Differentially expressed genes (DEGs) were screened and annotated by inputting the gene count matrix into DeSeq2. The normalized gene counts were used to conduct PCA and generate expression heatmaps. MA-plots of features were produced by plotting counts against fold changes (FCs). Genes with an FC > 2 and an FDR < 0.05 were subject to Gene Ontology (GO, http://geneontology.org/) analysis to study the alterations in biological process (BP), cellular component (CC), and molecular function (MF). The top GO terms were visualized using GOCluster and GOChord programs in GOplot package (Walter et al., 2015). In addition, Kyoto Encyclopedia of Genes and Genomes (KEGG) analysis was performed using the enrichKEGG program in the clusterProfiler package.

2.8. Integrated analysis

The identified significant metabolites were mapped to the *S.* Typhimurium (taxonomy: 99287) metabolic network in the KEGG database, and the genes involved in metabolic reactions were collected and aligned with the transcriptional profiles obtained from the RNA-seq data. DEGs that did not participate in the metabolic network were manually examined and clustered according to their biological functions. Their function roles in EO adaptation were further integrated in the mechanism illustration.

2.9. Quantitative real-time reverse transcription PCR validation

Quantitative real-time reverse transcription PCR (qRT-PCR) analysis of selected genes in three *S.* Typhimurium strains (ATCC 14028, ATCC 51812, and ATCC 25241) under MIC_{50} Thy and MIC_{50} Cin stress was conducted to verify the transcriptional conclusions. The culture, EO treatment, and RNA extraction of three strains were conducted as mentioned above. cDNA samples were synthesized using the obtained RNA as templates. The 16S rRNA gene (forward primer: 5′-CGGGGAGGAAGGTGTTGTG-3′, reverse primer: 5′-GAGCCCGGGGATTTCACATC-3′) was used as the reference gene (Dong et al., 2021). The specific primers used in this work were obtained from former studies

(Supplementary material 1) (Arunima et al., 2020a,b; Di Pasqua et al., 2013; Mühlig et al., 2014; Tsai et al., 2016). The qRT-PCR reaction was conducted according to our previous study (Chen et al., 2020). Three independent biological replicates were prepared, and each biological replicate represented three independent technical replicates.

2.10. Statistical analysis

Data were analyzed statistically using analysis of variance (ANOVA), and means were compared using the least significant difference (LSD) in SPSS (Version 22.0, IBM Corp., Armonk, NY, USA). Differences with a P value < 0.05 were considered significant.

3. Results and discussion

3.1. MIC test and GC–MS analysis of selected EOs

The MIC test of five EOs showed that garlic, ginger, and fennel oils did not inhibit the growth of *S.* Typhimurium at the highest test concentration (10 mg/mL). However, EOs Thy and Cin exhibited same MIC values (0.63 mg/mL) against *S.* Typhimurium. Previous studies showed similar MICs (from 0.32 to 1 mg/mL) for Thy and Cin against *Salmonella* serovars or *E. coli* (Boskovic et al., 2017; Zhang et al., 2016). Therefore, Thy and Cin oils were selected for further study.

The compositions of Thy and Cin were analyzed by GC–MS. In total, 12 and 16 compounds were identified in Thy (Table 1) and Cin (Table 2), respectively. In Thy, the erpenes cymene and thymol are the major volatile components. Bagamboula et al. (2004) reported that Thy comprises 45–47% thymol and 32–34% cymene. Similar contents of thymol (31.74%) and cymene (33.67%) were detected in the present study. Moreover, 12.48% γ-terpinene and 6.24% linalyl acetate were present in Thy. It has been reported that thymol is the major antibacterial component in Thy, while cymene shows weak antibacterial effects on certain bacteria (e.g., *Staphylococcus aureus*) (Bagamboula et al., 2004; Höferl et al., 2009). In addition, some compounds (e.g., linalyl acetate, 4-carvomenthenol, and pinene) with relatively lower contents, also present antimicrobial properties to different degrees (Swamy et al., 2016).

Table 1
Gas chromatography–mass spectrometry analysis of a thyme oil sample.

No.	RT (min)[a]	Name	Formula	CAS No.	Relative Content (%)
1	2.35	(1R,5R)-α-pinene	$C_{10}H_{16}$	7785–70-8	4.23 ± 0.89
2	2.50	2,2-Dimethyl-3-methylenenorbornane	$C_{10}H_{16}$	79–92-5	1.33 ± 0.31
3	2.70	(1S)-(-)-β-Pinene	$C_{10}H_{16}$	18172–67-3	1.61 ± 0.27
4	3.12	o-Cymene	$C_{10}H_{14}$	527–84-4	33.67 ± 3.55
5	3.49	γ-Terpinene	$C_{10}H_{16}$	99–85-4	12.48 ± 1.96
6	3.96	Linalyl acetate	$C_{12}H_{20}O_2$	115–95-7	6.24 ± 1.17
7	4.87	D-Camphor	$C_{10}H_{16}O$	464–49-3	2.27 ± 0.54
8	5.13	Isocamphol	$C_{10}H_{18}O$	124–76-5	0.82 ± 0.22
9	5.26	Isoborneol	$C_{10}H_{18}O$	507–70-0	1.61 ± 0.15
10	5.39	4-Carvomenthenol	$C_{10}H_{18}O$	562–74-3	1.33 ± 0.21
11	7.49	Thymol	$C_{10}H_{14}O$	89–83-8	31.74 ± 2.58
12	10.88	Bicyclo[5.2.0]nonane, 2-methylene-4,8,8-trimethyl-4-vinyl-	$C_{15}H_{24}$	242794–76-9	2.68 ± 0.34

[a] Retention time.

Table 2
Gas chromatography–mass spectrometry analysis of a cinnamon oil sample.

No.	RT (min)[a]	Name	Formula	CAS No.	Relative Content (%)
1	2.50	2,2-Dimethyl-3-methylenenorbornane	$C_{10}H_{16}$	79–92-5	0.39 ± 0.10
2	2.72	4(10)-Thujene	$C_{10}H_{16}$	3387–41-5	0.38 ± 0.12
3	2.95	α-Fellandrene	$C_{10}H_{16}$	99–83-2	1.29 ± 0.35
4	3.05	α-Terpinene	$C_{10}H_{16}$	99–86-5	0.60 ± 0.14
5	3.13	o-Cymene	$C_{10}H_{14}$	527–84-4	3.56 ± 0.88
6	3.22	β-Phellandrene	$C_{10}H_{16}$	555–10-2	3.56 ± 0.79
7	3.96	Linalyl acetate	$C_{12}H_{20}O_2$	115–95-7	2.45 ± 0.75
8	5.40	4-Carvomenthenol	$C_{10}H_{18}O$	562–74-3	0.19 ± 0.04
9	5.64	L-α-Terpineol	$C_{10}H_{18}O$	10482–56-1	0.35 ± 0.01
10	7.27	Cinnamaldehyde	C_9H_8O	14371–10-9	61.35 ± 4.98
11	9.04	Eugenol	$C_{10}H_{12}O_2$	97–53-0	9.16 ± 0.92
12	9.73	Copaene	$C_{15}H_{24}$	3856–25-5	1.22 ± 0.14
13	10.88	Bicyclo[5.2.0]nonane, 2-methylene-4,8,8-trimethyl-4-vinyl-	$C_{15}H_{24}$	242794–76-9	7.75 ± 1.54
14	11.44	Cinnamyl acetate	$C_{11}H_{12}O_2$	103–54-8	5.48 ± 0.85
15	11.81	α-Humulene	$C_{15}H_{24}$	6753–98-6	1.37 ± 0.27
16	15.19	Caryophyllene oxide	$C_{15}H_{24}O$	1139–30-6	0.90 ± 0.21

[a] Retention time.

Cin mainly consisted of cinnamaldehyde, which comprised 61.35% of the total relative content (Table 2), followed by eugenol (9.16%), 2-methylene-4,8,8-trimethyl-4-vinyl-bicyclo[5.2.0]nonane (7.75%), cinnamyl acetate (5.48%), and others. A previous study showed that in Cin extracted from bark, cinnamaldehyde is the major substance, with a content ranging from 62 to 90% (Nabavi et al., 2015). Our results agree with this conclusion. Moreover, eugenol is the main component in Cin extracted from leaves. Cinnamaldehyde and eugenol are important compounds contributing to the antibacterial effects of Cin (Nabavi et al., 2015). Fraňková et al. (2014) reported that the MICs of Cin against *Cronobacter sakazakii* and *C. malonaticus* were similar to that of pure cinnamaldehyde, while eugenol presented higher MIC values. This implied that cinnamaldehyde has stronger antibacterial activity compared with eugenol.

3.2. Growth kinetics under sublethal EO stresses

The 16 h growth kinetics of *S.* Typhimurium in the presence of 0.31 mg/mL (MIC_{50}) Thy or Cin were monitored (Fig. 1) and the growth parameters are summarized in Table 3. In the control, the lag phase and maximum growth rate were 2.16 h and 1.80 h^{-1}, respectively. The lag phase represents the time needed to repair injury and return to normal cell conditions, which enables microorganisms to proliferate (Wesche et al., 2009). However, a significantly longer lag phase was observed in the cells treated with MIC_{50} Thy (2.88 h) and MIC_{50} Cin (4.75 h) ($P < 0.05$). Furthermore, the maximum growth rate was significantly decreased to 1.26 h^{-1} in the MIC_{50} Cin group ($P < 0.05$) (Table 3). Similarly, Mazzarrino et al. (2015) observed extended lag phases during the growth of *S.* Typhimurium and *L. monocytogenes* cultured in medium containing different EOs. Moreover, lower growth rates of *S.*

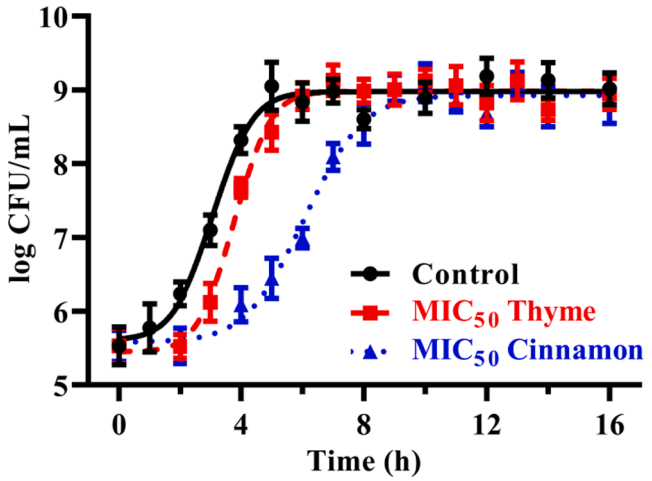

Fig. 1. Growth curves of *S.* Typhimurium grown in TSB containing 2.5% (v/v) ethanol (control), 0.31 mg/mL thyme oil, or 0.31 mg/mL cinnamon oil for 16 h at 37 °C.

Table 3
Growth parameters of *S.* Typhimurium cultured in TSB containing 2.5% (v/v) ethanol, 0.31 mg/mL thyme, or 0.31 mg/mL cinnamon oil.

Treatment[a]	Growth parameters[b]			
	Initial cell density (log CFU/mL)	Lag phase duration (h)	Maximum growth Rate (h^{-1})	Final cell density (log CFU/mL)
Control	5.62 ± 0.42A	2.16 ± 0.14C	1.80 ± 0.12 A	9.00 ± 0.33 A
MIC_{50} Thy	5.44 ± 0.37 A	2.88 ± 0.27B	1.90 ± 0.25 A	9.10 ± 0.31 A
MIC_{50} Cin	5.58 ± 0.54 A	4.75 ± 0.69 A	1.26 ± 0.11B	8.94 ± 0.45 A

[a] Control, 2.5% (v/v) ethanol; MIC_{50} Thy, 0.31 mg/mL thyme oil; MIC_{50} Cin, 0.31 mg/mL cinnamon oil.
[b] Different uppercase letters in the same column represent significant differences ($P < 0.05$) among three groups.

Typhimurium in the presence of sublethal terpenes were reported by Dubois-Brissonnet et al. (2011). The lower growth rates of *S.* Typhimurium under EO stress might be associated with greater resistance because of the increased expression of stress related proteins (Yuan et al., 2018).

3.3. Direct and cross-resistance

To confirm whether sublethal EO exposure led to measurable resistance, *S.* Typhimurium cells cultured in MIC_{50} Thy and MIC_{50} Cin were challenged by lethal treatments, including acid (SGF, pH 1.5), heat (58 °C), oxidant (H_2O_2, 50 mM), Thy (0.63 mg/mL), or Cin oil (0.63 mg/mL). The induced stress resistances, as represented using D values, are shown in Table 4. In the human body, acidic gastric fluid plays an important role in the defense against foodborne pathogens. The results showd that, compared with the control, no significant differences in SGF resistance were observed in the EO adapted groups. The D values in three groups were all around 7 min (Table 4). Yuan et al. (2018) also reported a lack of induced acid tolerance in *E. coli* O157:H7 after exposure to thymol and cinnamaldehyde, which are major constituents of Thy and Cin oils, respectively. To survive under acid stress, *S.* Typhimurium has evolved complex AR systems, namely, AA-dependent decarboxylase/antiporter systems, F_1-F_0 ATPase, and modifications of the cell membrane (Lund et al., 2014). EO stress might not induce the AR-related systems, and this hypothesis will be further examined in the following metabolomic and transcriptomic analyses.

Table 4
D values of non-adapted, and thyme or cinnamon oil adapted, *S.* Typhimurium treated with acid, thermal, hydrogen peroxide, thyme, or cinnamon oil.

Treatment	D values (min)[b]		
	Control	MIC_{50} Thy	MIC_{50} Cin
Acid (SGF[a], pH 1.5)	7.14 ± 0.54 A	7.80 ± 0.63 A	6.75 ± 0.89 A
Thermal (58 °C)	4.57 ± 0.66C	26.88 ± 3.57 A	14.77 ± 1.24B
Hydrogen peroxide (50 mM)	12.89 ± 0.97B	45.25 ± 4.26 A	51.55 ± 8.31 A
Thy (0.63 mg/mL)	3.65 ± 0.45B	6.87 ± 1.21 A	4.12 ± 0.62B
Cin (0.63 mg/mL)	81.22 ± 8.21C	117.59 ± 9.74B	215.42 ± 12.58 A

[a] SGF, simulated gastric fluid.
[b] Different uppercase letters in the same row represent significant differences ($P < 0.05$) among three groups.

D values for thermal treatment (58 °C), as shown in Table 4, demonstrated that both adapted groups presented significantly stronger thermal resistance (26.88 and 14.77 min in the MIC_{50} Thy and MIC_{50} Cin groups, respectively; $P < 0.05$) compared with that of the non-adapted control (4.57 min). Similarly, the EO-adapted cells displayed significantly enhanced resistance (D values, around 50 min) against oxidative stress, compared with that in the control (12.89 min) ($P < 0.05$). It is widely accepted that pore formation and subsequent oxidative stress contribute to the antibacterial effects of EOs (Kovács et al., 2016). For instance, the expression levels of oxidative stress response genes (*sodA* and *soxR*) were increased significantly in *E. coli* after exposure to cinnamaldehyde, which is the major component of Cin (Visvalingam et al., 2013). Therefore, the MIC_{50} Thy and MIC_{50} Cin treatments might induce the antioxidant response in *S.* Typhimurium cells, resulting in improved survival abilities in 50 mM H_2O_2.

The resistances of EO-adapted *S.* Typhimurium against lethal levels of Thy and Cin oils were also determined (Table 4). The D values of Thy and Cin to kill 90% non-adapted cells were 3.65 ± 0.45 and 81.22 ± 8.21 min, respectively, indicating the greater sanitizing effect of Thy oil. Pei et al. (2009) reported that thymol and cinnamaldehyde exhibited similar antibacterial effects against *E. coli*. Therefore, other compounds (e.g., γ-terpinene) in Thy might contribute to the improved antimicrobial activity (Table 1). *S.* Typhimurium adapted to MIC_{50} Thy presented more resistant to subsequent Thy (6.87 min) and Cin (117.59 min) treatments. However, cells adapted to MIC_{50} Cin only developed direct-resistance to Cin treatment (215.42 min). Similarly, *Bacillus cereus* exhibited enhanced survival under lethal carvacrol stress after exposing to sublethal levels of carvacrol (5). To date, limited information about the EO adaptation mechanism is available because of the complex antibacterial targets of EOs.

3.4. Metabolomics analysis

The overall metabolic responses of *S.* Typhimurium exposed to sublethal levels of Thy and Cin were studied using UPLC-QTOF-MS. PCA showed that the replicates in each group were aggregated, and the three groups were well separated (Fig. 2A). The results indicated that Thy and Cin might induce different metabolic responses. MS profiles exhibited 30,199 features with their normalized intensities in the three groups (Supplementary material 2). The intensity profiles of the pairwise comparisons (control *vs.* MIC_{50} Thy; control *vs.* MIC_{50} Cin; MIC_{50} Thy *vs.* MIC_{50} Cin) were subject to supervised OPLS-DA to screen the significant features. The S-plots in Fig. 2B-D show the VIP features in each paired comparison. Compared with the control group, MIC_{50} Thy treatment induced 2501 significantly changed features, while MIC_{50} Cin induced more changed features (3138, supplementary material 2). In the pairwise comparison MIC_{50} Thy *vs.* MIC_{50} Cin, 2063 notable features were screened.

The screened VIP features were identified based on MS/MS spectra, related databases, and references. In total, 47 metabolites including

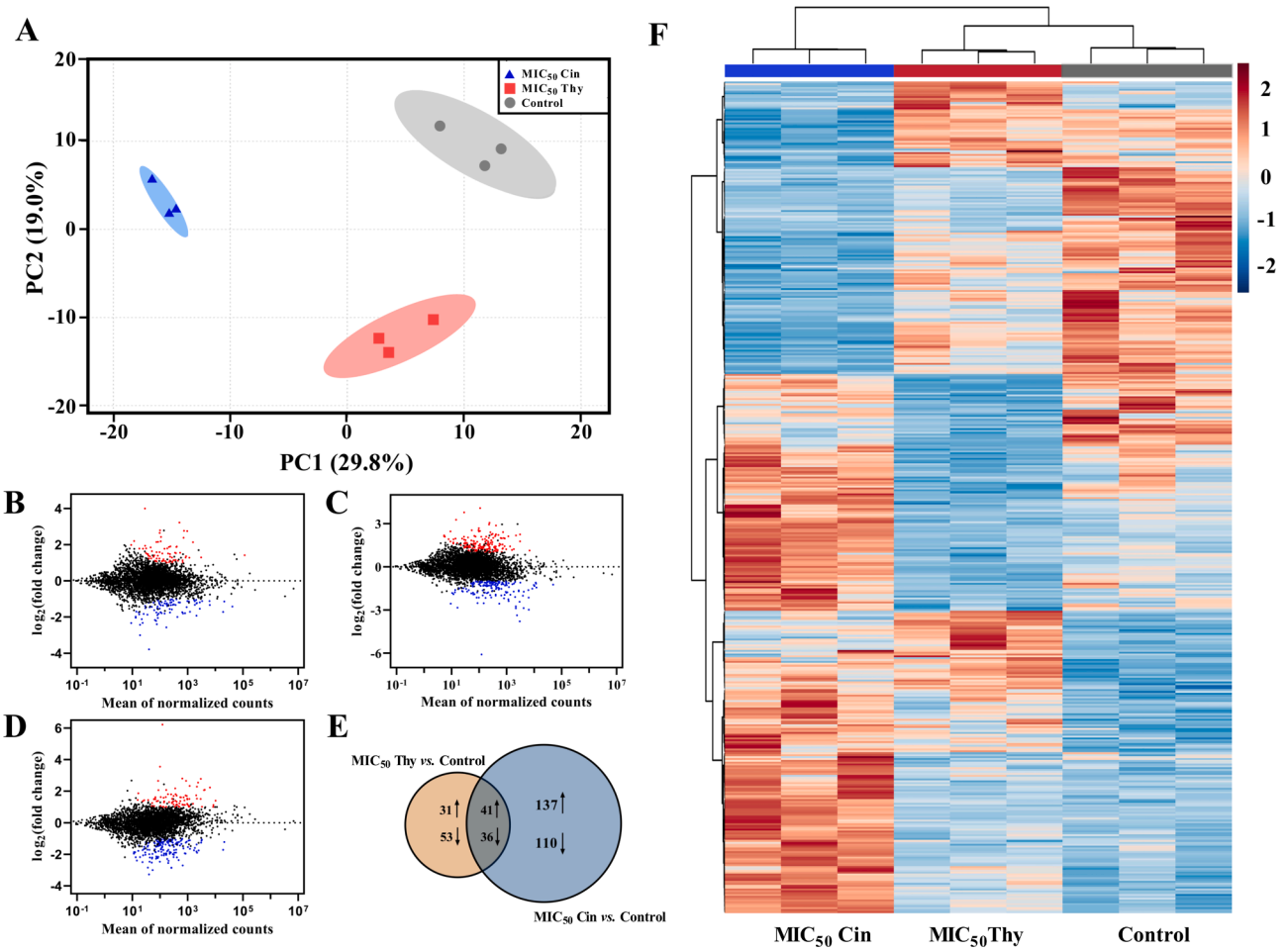

Fig. 2. (A) Principal component analysis (PCA) score plot of the intracellular metabolic profiles of the three groups; (B) S-plot of pairwise comparison control *vs.* MIC_{50} Thy. Red dots represent the significant features (VIP > 1, FDR < 0.05) screened from orthogonal partial least squares discriminant analysis (OPLS-DA); (C) S-plot of pairwise comparison control *vs.* MIC_{50} Cin; (D) S-plot of pairwise comparison MIC_{50} Thy *vs.* MIC_{50} Cin; (E) Venn diagram showing the overlap of significant metabolites between the group control *vs.* MIC_{50} Thy and control *vs.* MIC_{50} Cin; (F) Heatmap of 54 identified metabolites in the three groups. In MetaboAnalyst 5.0, the data were normalized by sum, and processed by logarithmic transformation and Pareto scaling. Group clustering was conducted using the Ward algorithm. Default color contrast was applied, and the color bar was standardized using the autoscale feature method. Note: NRC, nucleotide-related compound; OA, organic acid. (For interpretation of the references to color in this figure legend, the reader is referred to the web version of this article.)

lipids, oligopeptides, amino acids (AAs), nucleotide related compounds (NRCs), and organic acids (OAs) were identified (Fig. 2F, supplementary material 2). The contents of 8 intracellular metabolites increased in both EO treated groups, while the levels of 33 metabolites decreased (Fig. 2E). Lipids and related compounds 1–5 presented higher concentrations in the control. By contrast, the synthesis of lipid compounds were enhanced significantly (by 6–8 fold) in the EO-treated groups. Lipid metabolites, including phospholipids, glycolipids, and fatty acids, are associated closely with stress adaptation and cell fitness maintenance (Rowlett et al., 2017; Giotis et al., 2007). For instance, *L. monocytogenes* adapts effectively to mild or moderate pH stress by regulating the proportions of branched-chain fatty acids (Giotis et al., 2007). Our study showed that lipid transformation occurred and contributed to the EO stress adaptation of *S.* Typhimurium.

Bacteria internalize oligopeptides from the extracellular environment using ATP–binding cassette transporters to sustain their nutritive demand and biological synthesis. For *Salmonella*, peptide transportation might be the main pathway providing the AAs required for survival inside the host and the establishment of infection (Garai et al., 2017). Our results showed that most of the detected oligopeptides were degraded to meet the AA requirements of *S.* Typhimurium under the EO treatments (Fig. 2F, Dupplementary material 2). AA metabolism is complex and vital during stress adaptation. For example, during the exponential growth of *E. coli*, glutamic acid is a key metabolite, accounting for around 40% of total intracellular metabolites. Moreover, glutamic acid-related metabolism plays important roles in bacterial stress tolerance, such as that to acid, metal, and oxidation (Ramond et al., 2014; Djoko et al., 2017). Our results showed that glutamic acid levels were notably increased (VIP > 1, FDR < 0.05), by 1.85 and 2.25 fold, in the MIC_{50} Thy and MIC_{50} Cin groups, respectively (Fig. 2F, supplementary material 2), implying its crucial role during EO adaptation. Metabolic analysis also showed significantly altered contents of some NRCs during the EO adaptation of *S.* Typhimurium (Fig. 2F, supplementary material 2). The notable changes in these NRCs implied that EOs might accelerate nucleotide turnover, which could indicate increased levels of DNA damage (Belenky et al., 2015).

The enrichment analysis was conducted, as shown in Fig. 3A, based on the screened significant metabolites (VIP > 1, FDR < 0.05). In total, 14 metabolic pathways were altered significantly ($P < 0.05$) (Supplementary material 3). Aminoacyl-tRNA biosynthesis, which provides AA donors for protein translation, was the most affected metabolic pathway. Moreover, 10 significant AA metabolic pathways could provide substrates for aminoacyl-tRNA biosynthesis (Bullwinkle & Ibba, 2016). Therefore, altered protein synthesis might be induced by sublethal EO treatments. The pairwise pathway analyses are shown in Fig. 3B-D and supplementary material 3. Sublethal Thy treatment resulted in 12

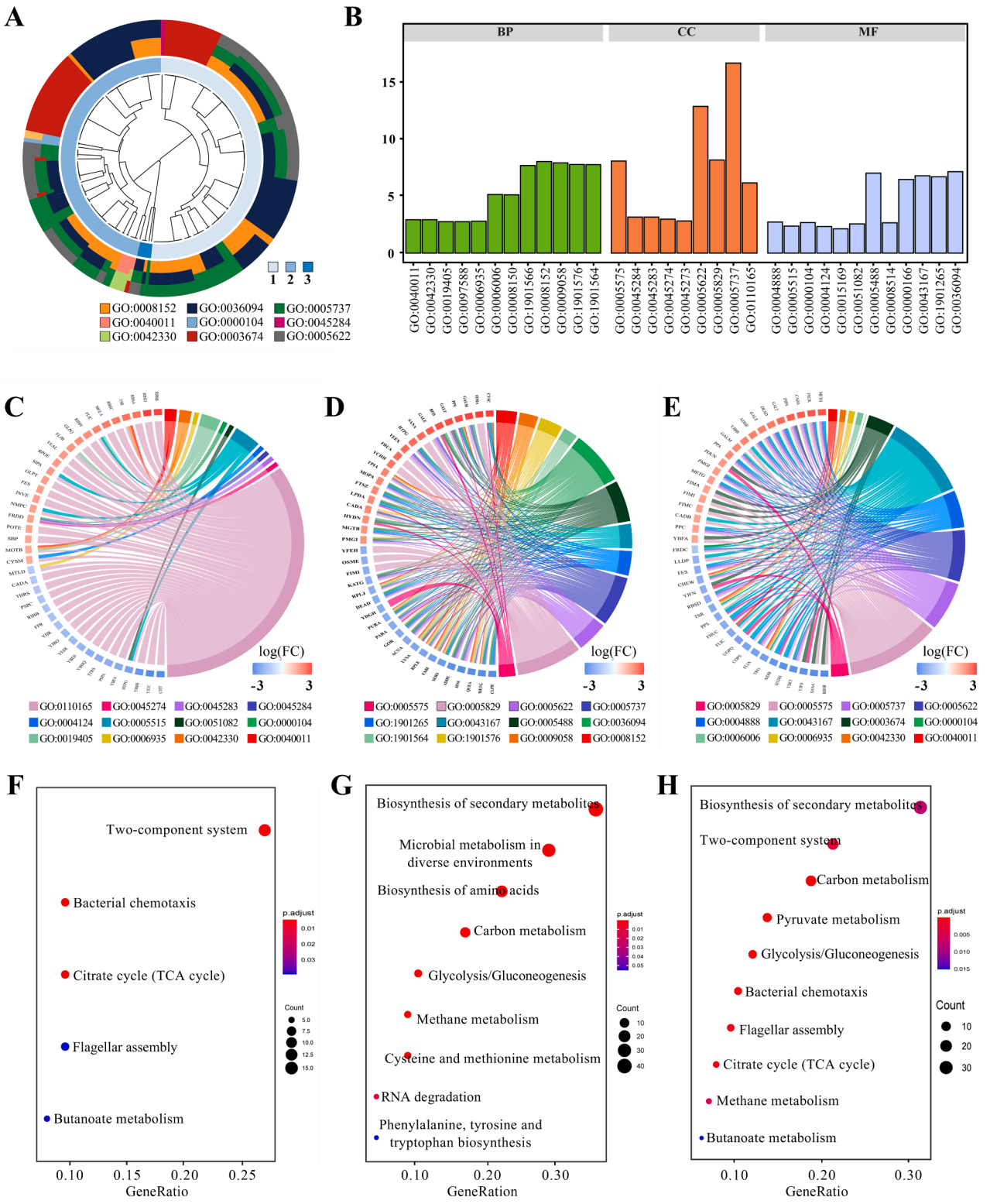

Fig. 3. Metabolite pathways analysis. (A) Pathway enrichment pathway analysis showing the top 25 affected pathways with their significant metabolites. Numbers 1–3 represent the times of each metabolite detected in three pairwise groups. The color bar was scaled using the *P* values of the metabolic pathways; (B) Pathway analysis of the pairwise comparison control *vs.* MIC_{50} Thy; (C) Pathway analysis of the pairwise comparison control *vs.* MIC_{50} Cin; (D) Pathway analysis of the pairwise comparison MIC_{50} Thy *vs.* MIC_{50} Cin.

significantly up or down-regulated pathways ($P < 0.05$). Glutamine and glutamate metabolism, purine metabolism, and arginine and proline metabolism, were markedly altered, indicating their important roles during adaptation. Previous studies also showed significant alterations of these pathways in bacteria under stresses, such as electrolyzed water, ultrasound, and acid (Chen et al., 2020; Liu et al., 2017; Zhao et al., 2019). Similarly, MIC_{50} Cin induced pathways such as aminoacyl-tRNA biosynthesis, and suppressed the arginine and proline metabolism. The different pathways between MIC_{50} Thy and MIC_{50} Cin adapted cells (Fig. 3D) revealed their different adaptive mechanisms.

3.5. Transcriptomics analysis

The comprehensive transcriptional responses of *S.* Typhimurium treated with sublethal Thy and Cin were studied using RNA-seq. PCA discriminated the three groups at the transcriptional level (Fig. 4A). In total, 3928 genes were mapped to the reference *S.* Typhimurium genome (NC_003197) (Supplementary material 4). In addition, the MA plots, shown in Fig. 4B-D, present the gene expression patterns in pairwise groups. Genes, including *rnpB*, *sopD*, *lpp*, and *csrB*, exhibited high mean counts ($>10^5$) in the three groups, indicating their important roles in *S.* Typhimurium's basic physiological activities. For example, the gene *sopD*, encoding an effector protein, is involved in the *Salmonella* type III secretion system (T3SS). It might also play an important role in the development of antibiotic resistance (Khoo et al., 2015). The heatmap presented in Fig. 4F, shows the expression patterns of DEGs with FC > 2 and FDR < 0.05. In the pairwise comparison, control *vs.* MIC_{50} Thy, 161 DEGs were identified (Supplementary material 4), and their biological functions were annotated in supplementary material 5. Moreover, MIC_{50} Cin treatment resulted in 324 DEGs, indicating more reactive responses during Cin adaptation compared with those induced during Thy adaptation. The 260 DEGs identified between the MIC_{50} Thy and MIC_{50} Cin treatments further confirmed their different adaptive mechanisms.

In the pairwise comparison, control *vs.* MIC_{50} Thy, 161 genes were significantly altered (FC > 2, FDR < 0.05) (Supplementary material 4). Top 10 up-regulated genes (*citT*, *yjcC*, *ybhS*, *ypeC*, *htpG*, *ybfA*, *pspA*, *ttrS*, *ybhQ*, and *rspA*) are involved in various physiological activities. For example, the gene *ttrS* controls the expression of *ttr*, which is a component of T3SS that facilitates pathogenesis (Edrees et al., 2018). The genes *citT* and *ybhS*, both encoding permeases, that function to translocate various nutrients across biological membranes (Garai et al., 2017). By contrast, the top 10 down-regulated genes (Supplementary material 4; including *rbsB*, *rbsD*, *rbsA*, *rbsC*, and *mglA*) are responsible for synthesizing the transporters of ribose and galactose/methyl galactoside. These results implied that the uptake of ribose and galactose/methyl galactoside were compromised by MIC_{50} Thy treatment.

Compared with Thy treatment, adaptation to Cin treatment resulted in more DEGs (Supplementary material 4). Some of the top altered genes (e.g., *citT*, *htpG*, and *ribH*) exhibited similar expression patterns under the two EO treatments. However, the expression levels of some genes, such as *pspA* and *fliC*, were only significantly altered under MIC_{50} Thy treatment. In the pairwise comparison, control *vs.* MIC_{50} Cin, some different DEGs were listed in top 10 up and down-regulated genes. For

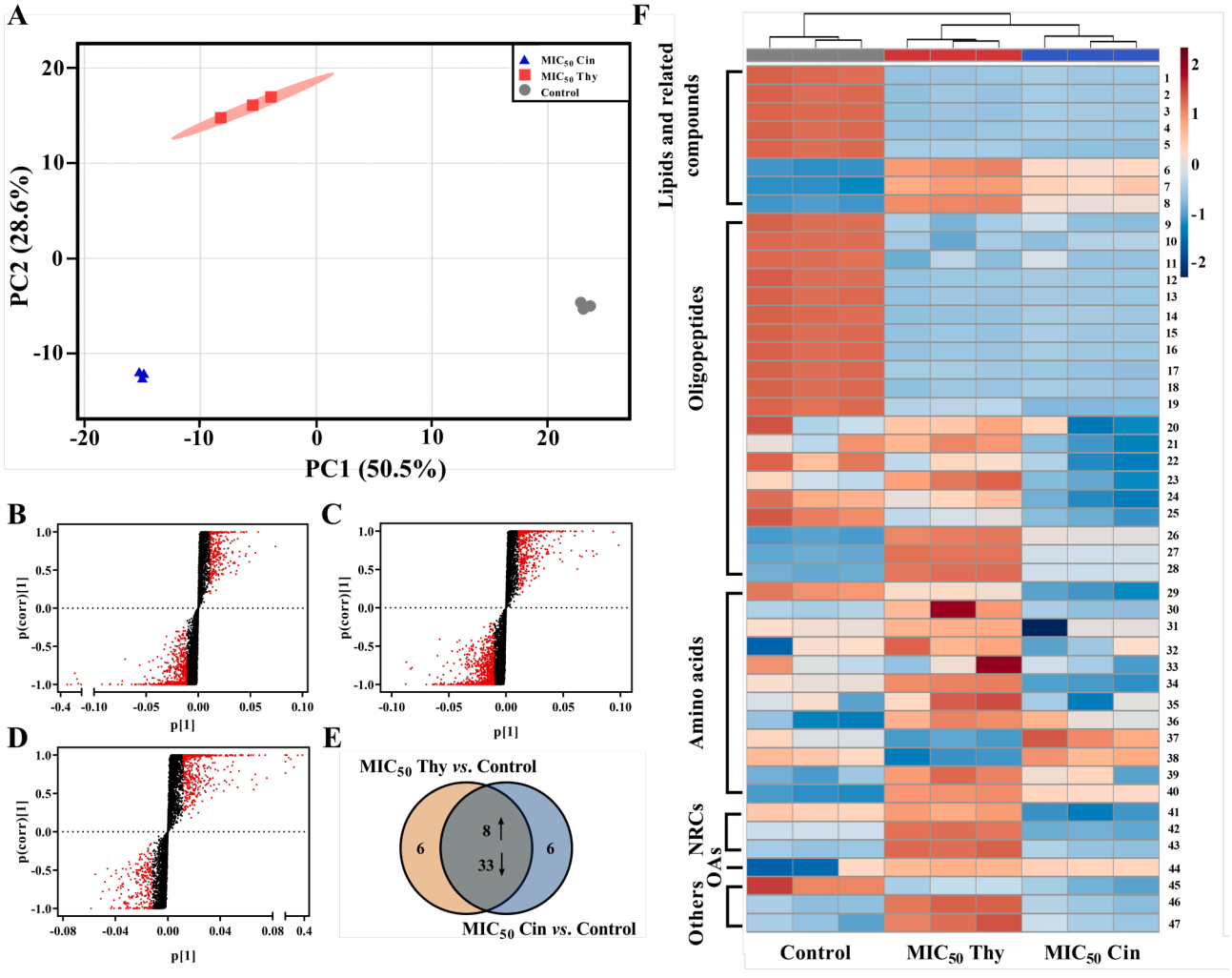

Fig. 4. Differentially expressed genes analysis. (A) Principal component analysis (PCA) score plot of the transcriptional profiles of the three groups; (B) MA-plot of the pairwise comparison control *vs.* MIC_{50} Thy. Red and blue dots represent the significantly (Fold change, FC > 2, FDR < 0.05) upregulated and downregulated genes, respectively; (C) MA-plot of the pairwise comparison control *vs.* MIC_{50} Cin; (D) MA-plot of the pairwise comparison MIC_{50} Thy *vs.* MIC_{50} Cin; (E) Venn diagram showing the overlap of significant genes between the control group *vs.* MIC_{50} Thy and control *vs.* MIC_{50} Cin; (F) Heatmap of differentially expressed genes (FC > 2, FDR < 0.05) in the three groups. In MetaboAnalyst 5.0, the data were normalized by sum, and processed by logarithmic transformation and Pareto scaling. Group clustering was conducted using the Ward algorithm. Default color contrast was applied, and the color bar was standardized by the autoscale feature method. (For interpretation of the references to color in this figure legend, the reader is referred to the web version of this article.)

instance, *pps*, encodes a phosphoenolpyruvate synthase that participates in glycolysis and gluconeogenesis in *S.* Typhimurium. The notable differences in altered gene number and function between MIC_{50} Thy and MIC_{50} Cin treatments indicated the different adaptive responses of *S.* Typhimurium cells.

GO enrichment analysis was conducted to investigate the functions of the screened DEGs (Fig. 5, supplementary material 6). During Thy adaptation, BP locomotion (GO:0040011), which is defined as self-propelled movement of a cell, was the most affected (Fig. 5A). By contrast, GO terms metabolic process (GO:0008152), cytoplasm (GO:0005737), and small molecule binding (GO:0036094) were remarkably affected by Cin, indicating that transmembrane material exchange and related intracellular metabolism were induced strongly by Cin. More top GO terms induced during EO adaptation are shown in Fig. 5B. For instance, chemotaxis (GO:0006935) and fumarate reductase complex (GO:0045283), were highlighted. The correlations between the top altered genes and GO terms were examined using GOChord analysis (Fig. 5C-E). In the pairwise comparison, control *vs.* MIC_{50} Thy, all the selected genes were associated with the CC cellular anatomical subgroup (GO:0110165). This implies that intracellular metabolism and biological synthesis were induced strongly during Thy adaptation. By contrast, during Cin adaptation, genes, such as *metG* and *hns*, correlated with CC GO:0005829 (cytosol). Thus, these genes might participate in certain cytosolic activities.

KEGG analysis was performed to study the metabolic pathways related to the DEGs (Fig. 5F-H and Supplementary material 6). During Thy adaptation, five pathways, including two-component system, bacterial chemotaxis, TCA cycle, flagellar assembly, and butanoate metabolism, were affected significantly ($P < 0.05$) (Fig. 5F). The enriched pathways in the control *vs.* MIC_{50} Cin group are shown in Fig. 5G. Nine metabolic pathways, including methane metabolism and glycolysis/gluconeogenesis, were altered markedly ($P < 0.05$). The results indicated that some basic metabolisms, such as sugar metabolism, AA metabolism, and carbon metabolism, are involved in Cin adaptation. The pathway differences between MIC_{50} Thy and MIC_{50} Cin treatments are presented in Fig. 5H. The enriched pathways were almost represented by the combined pathways shown in Fig. 5F and Fig. 5G. This further showed the distinct adaptation mechanisms of *S.* Typhimurium against Thy and Cin EOs.

3.6. Integrated omics analysis

To comprehensively investigate the molecular mechanisms of EO adaptations in *S.* Typhimurium, integrated analysis was conducted and the speculative molecular mechanisms are summarized in Fig. 6. *S.* Typhimurium cells adopted a conservative strategy to survive under harsher Thy stress (Fig. 6A), as evidenced by the significantly lower D value ($P < 0.05$) compared with that under Cin treatment (Table 4). Cell motility was inhibited because of the downregulation of genes involved in flagellar assembly (*flgK*, *flgL*, *fliC*, *motB*, and *fljB*) and chemotaxis (*cheA*, *cheW*, *cheM*, and *tsr*) (Jarrell & Albers, 2012). Moreover, transmembrane material exchange was strongly compromised. The genes encoding proteins that involves in the translocation of sugar (*mglA*, *cboQ*, *fhuC*, *glpT*, and *manZ*), AAs (*sbp*, *argT*, *dcuA*, and *sdaC*), dipeptides (*dppF*), and other small molecules (*ompC* and *nmpC*), were significantly downregulated (FC > 2, FDR < 0.05) (Tanaka et al., 2018). Thus, *S.*

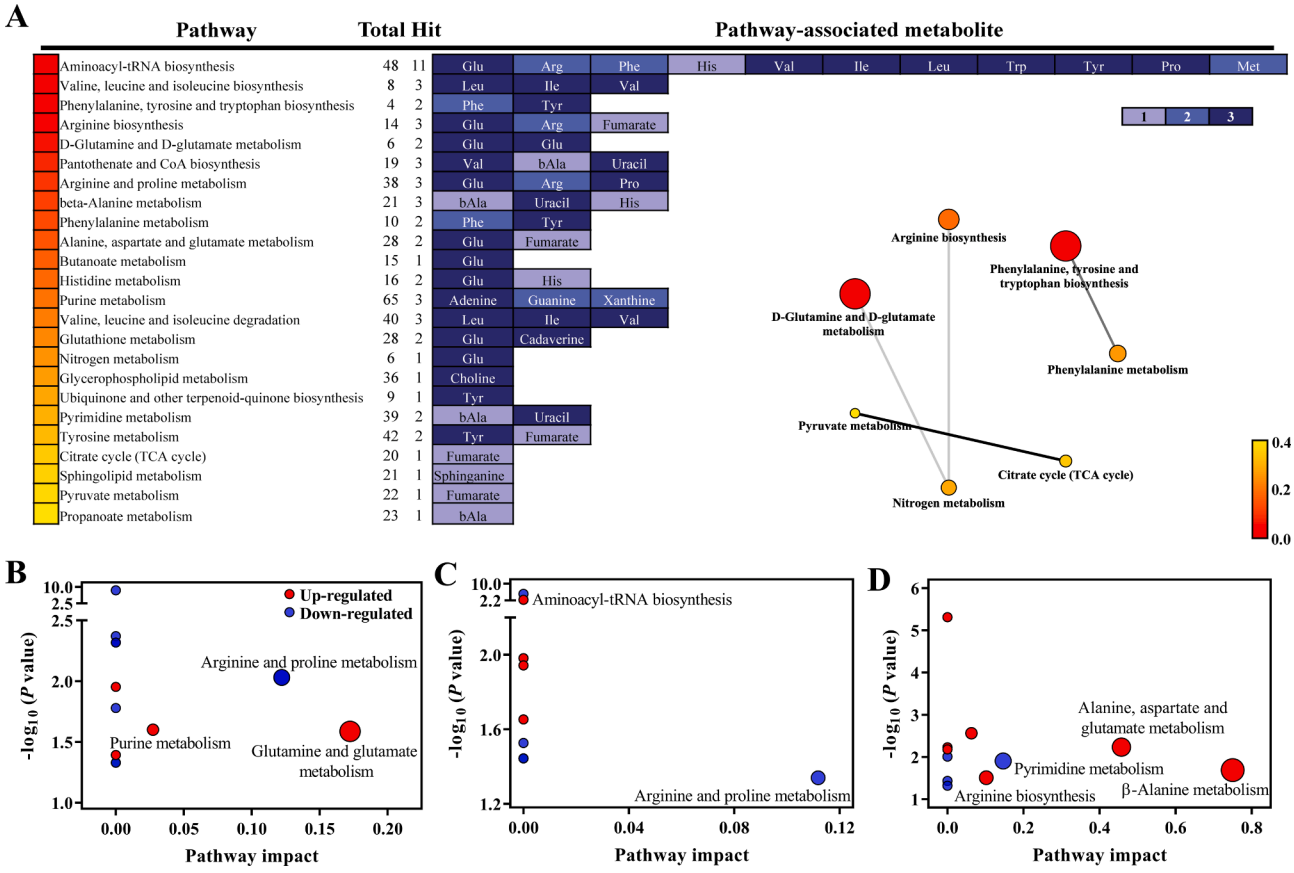

Fig. 5. Functional analysis of DEGs. (A) A circular dendrogram showing the expression spectrum clustering. The inner ring represents the screened differentially expressed genes (DEGs) colored by the times detected in three pairwise groups. The outer ring indicates the assigned functional gene ontology (GO) terms; (B) GO terms enrichment analysis showing the top terms involved in essential oil stress adaptation; (C-E) GOChord plot showing the correlation between the top DEGs and GO terms in the pairwise comparison control *vs.* MIC_{50} Thy, control *vs.* MIC_{50} Cin, and MIC_{50} Thy *vs.* MIC_{50} Cin; (F-H) KEGG pathway analysis in the pairwise comparison control *vs.* MIC_{50} Thy, control *vs.* MIC_{50} Cin, and MIC_{50} Thy *vs.* MIC_{50} Cin.

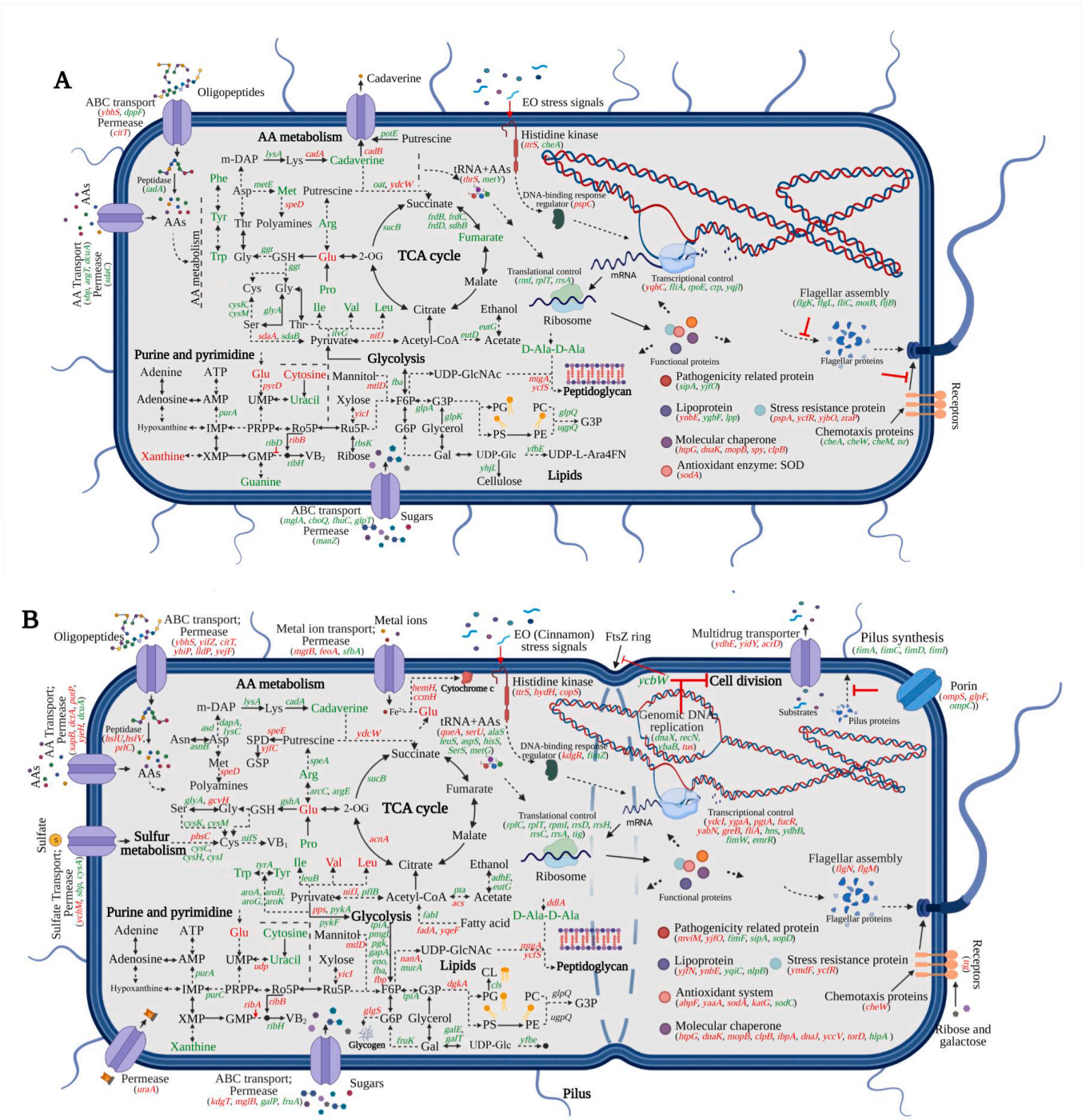

Fig. 6. The molecular mechanisms of *S.* Typhimurium cells during adaptation to sublethal concentrations of thyme (A) and cinnamon (B) oils. Genes or metabolites labeled in red indicate a significantly increased expression level or content in EO-treated cells, compared with those in the control group. By contrast, genes or metabolites labeled in green indicate a significantly decreased expression level or content in EO-treated cells. Note: EO, essential oil; AA, amino acid; SOD, superoxide dismutase; TCA, tricarboxylic acid; 2-OG, oxoglutaric acid; m-DAP, *meso*-diaminoheptanedioate; PG, phosphatidylglycerol; PS, phosphatidylserine; PC, phosphatidylcholine; PE, phosphatidylethanolamine;G3P, glycerophosphoric acid; ABC, ATP-binding cassette; SPD, spermidine; GSP, glutathionylspermidine; F6P, D-fructose 6-phosphate; G6P, D-glucose 6-phosphate; Gal, galactose. (For interpretation of the references to color in this figure legend, the reader is referred to the web version of this article.)

Typhimurium cells under MIC_{50} Thy treatment seem to adopt certain critical and fundamental strategies to survive and replicate.

Intracellular metabolic analysis of *S.* Typhimurium cells during Thy adaptation showed that sugar and lipid metabolisms were compromised. The related gene expression levels (e.g., *fba*, *glpK*, *glpQ*, and *yfbE*) and metabolite contents were downregulated. Nevertheless, purine and pyrimidine metabolisms were induced, and metabolites, including adenine, xanthine, and cytosine, accumulated (Fig. 6A). AA metabolism is crucial and complex in bacterial stress responses. Glutamic acid is accumulated from the transformation of other AAs such as proline and arginine (Chen et al., 2020). Sugar, AA, and lipid metabolisms might provide substrates for certain key functional compounds. For instance, dipeptide D-Ala-D-Ala was consumed, which participates in the synthesis of peptidoglycan and is further utilized for cell wall repair and the

cell envelope. Expression levels of *mtgA* and *ycfS*, encoding the key enzymes monofunctional biosynthetic peptidoglycan transglycosylase and L,D-transpeptidase, respectively, were notably induced (Mitchell & Silhavy, 2019). The degradation of oligopeptides and the transformation of related AAs provided substrates for the syntheses of functional proteins. For example, stress resistance proteins and molecular chaperones were massively synthesized. Furthermore, superoxide dismutase, encoded by *soda*, was induced to destroy superoxide anion radicals. Abundant studies have proved their important roles in bacterial resistance against environment stresses (Lima et al., 2013).

Compared with Thy adaptation, the adaptive responses to Cin in *S.* Typhimurium cells were more radical and active (Fig. 6B). Cell motility was enhanced via the increased syntheses of receptor (*trg*) sensing ribose and galactose, chemotaxis protein (*cheW*), and flagellin (*flgN*) (Jarrell & Albers, 2012). Transmembrane material exchange was strongly activated. For instance, the expression levels of transport proteins of oligopeptides, AAs, sugars, sulfates, metal ions, and other small molecules were altered significantly. The multidrug transporters, encoded by *ydhE*, *yidY*, and *acrD*, were also activated. They are major mechanisms underlying multidrug resistance, and can secrete antimicrobials and therapeutic drugs effectively (Lu et al., 2013). Interestingly, some physiological activities were inhibited during Cin adaptation. For example, genes coding pilus proteins ((*fimA*, *fimC*, *fimD*, and *fimI*)) were downregulated, indicating that the pilus synthesis was inhibited. Moreover, the expression of *ycbW*, encoding the FtsZ-binding component of the Z ring, was inhibited (Hale et al., 2011). Some genomic DNA replication related genes (*dnaX*, *recN*, and *ybaB*) were also downregulated. These results indicated that the cell division of sublethal Cin-treated cells was compromised. This was in consistent with the growth kinetics results, with the MIC_{50} Cin treatment resulting in the longest lag phase time (Table 3).

MIC_{50} Cin treatment also resulted in more complex intracellular metabolism. For instance, besides being a precursor of purine and pyrimidine metabolism, glutamic acid reacts with ferrous ions to form cytochrome *c*, which acts as an electron carrier in cellular energy transduction (Sanders et al., 2010). Moreover, glycolysis was inhibited, while gluconeogenesis related genes (*fbp* and *glgS*) were upregulated to produce glycogen. This implies the alteration of carbon metabolism in *S.* Typhimurium under EO stress (Alteri & Mobley, 2012). In addition, genes (*cysC*, *cysH*, and *cysI*) in sulfur metabolism, associated with the production of sulfur–containing AAs (e.g., cysteine), were suppressed (Grossoehme et al., 2011). Intracellular AAs are transported from the extracellular environment (e.g., by the products of *xapB*, *dctA*, and *putP*), or produced from oligopeptide hydrolysis (by the products of *hslU*, *hslV*, and *prlC*). Moreover, AA metabolism is utilized to synthesize functional compounds such as peptidoglycan and proteins (Fig. 6B). In addition, more genes encoding stress related proteins were upregulated during Cin adaptation. For instance, *ymdF* and *ycfR*, encoding the proteins YmdF and YcfR, respectively, were induced markedly. YmdF plays a role in the flagellum-dependent motility and general stress response of *S.* Typhimurium, while YcfR is a stress resistance protein involved in acid, heat, hydrogen peroxide, and cadmium stress responses (Arunima et al., 2020a,b; Zhang et al., 2007).

The integrated analysis might also help to explain the results of induced direct and cross-resistance (Table 4). Compared with non-adapted cells, higher levels oxidative and thermal resistance in EO adapted cells were observed. The increased expression of stress resistance proteins and antioxidant systems played a crucial role in the induced resistance. However, the D value results showed that sublethal EO treatment did not induce acid tolerance of *S.* Typhimurium cells. However, alterations to some acid resistance mechanisms were observed in the EO-treated cells. For example, the lysine decarboxylase system (*cadA* and *cadB*) was activated in Thy-treated cells (Chen et al., 2020). Moreover, the induced molecular chaperone DnaK (*dnaK*) and GroES (*mopB*) prevent toxic protein aggregation and ensure proteome integrity (Lund et al., 2014). One possible explanation for the lack of an induced AR is that *S.* Typhimurium cells have evolved multiple AR mechanisms. Therefore, the up and downregulation of one or two AR systems might not induce a physiological effect (Yuan et al., 2018). Furthermore, lysine-dependent AR is effective at moderate acidic pH. Hence, the SGF conditions (pH 1.5) used in the present study might be an extreme acid challenge for adapted *S.* Typhimurium cells to show a physiological effect. Therefore, the sublethal Thy and Cin adaptations cannot induce acid tolerance in *S.* Typhimurium.

3.7. qRT-PCR validation

qRT-PCR was conducted to verify the transcript expression patterns in three *S.* Typhimurium strains (Supplementary material 7). The five DEGs tested were from the MIC_{50} Thy or MIC_{50} Cin treatment froups, and are responsible for different physiological functions. The results for strain ATCC 14,028 confirmed the increased expression of genes related to protein protection (*htpG* and *clpB*) and lysine decarboxylase system (*cadA*), and decreased expression of *yqjI* (transcriptional regulator) and *pgtP* (major facilitator superfamily transporter), under MIC_{50} Thy treatment. Moreover, the expression patterns of *htpG*, *clpB*, *katG*, *sopD*, and *cadA* under MIC_{50} Cin treatment were consistent with the results of the transcriptomic analysis. The fold change values obtained from qRT-PCR were lower than those from the RNA-seq, indicating a wider dynamic range in the RNA-seq analysis. Similar results were observed by Yuan et al. (2018) and King et al. (2010). Generally, the expression patterns among the three strains exhibited similar up and down-regulations. The results implied that these strains might share similar molecular mechanisms to adapt to the sublethal EO stress. However, some DEGs (e.g., *sopD*) indicated the occurrence of strain-dependent variations. Thus, more *S.* Typhimurium strains should be analyzed to reveal more general molecular mechanisms.

Lastly, the different pathways, transcripts, and metabolites affected by Thy or Cin treatments implied that the combination of the two EOs might help to prevent the development of resistance. For example, the combined use of EOs (e.g., lemongrass and rosemary) synergistically increased the inactivation efficacies against different pathogenic and spoilage bacteria (e.g., *Staphylococcus sciuri* and *Pseudomonas hibiscicola*) (György et al., 2020). The molecular mechanism of the synergistic effects should be studied in a future work.

4. Conclusion

In the present study, *S.* Typhimurium was found to successfully develop direct and cross-resistances to subsequent EO, thermal, and oxidative stresses, after exposure to sublethal levels of Thy and Cin. Integrated metabolomic and transcriptomic analyses were applied to investigate the adaptive mechanisms. Multivariate analysis of the results of the omics studies showed significant differences in adaptive strategies under the two EO stresses. MIC_{50} Thy-treated cells adopted more conservative strategies: Cell motility and transmembrane material exchange were inhibited. Some intracellular metabolisms (e.g., glutamine and glutamate metabolism, and purine metabolism) were activated to provide substrates for the syntheses of key functional compounds, such as peptidoglycan and restress resistance proteins. By contrast, more active responses were observed in the MIC_{50} Cin group. For instance, cell motility and transmembrane material exchange were activated. The synthesis of some important components, such as cytochrome *c* and glycogen, was enhanced. However, cell division and pilus synthesis were inhibited. Similar to those in the Thy group, many stress resistance proteins were synthesized in *S.* Typhimurium cells under Cin treatment. These data provide valuable information related to the prevention of the development of resistance by *S.* Typhimurium.

CRediT authorship contribution statement

Lin Chen: Conceptualization, Methodology, Investigation, Software,

Resources, Visualization, Writing – original draft. **Xue Zhao:** Formal analysis, Investigation, Software. **Rui Li:** Writing – review & editing. **Hongshun Yang:** Conceptualization, Funding acquisition, Project administration, Supervision, Validation, Writing – review & editing.

Declaration of Competing Interest

The authors declare that they have no known competing financial interests or personal relationships that could have appeared to influence the work reported in this paper.

Acknowledgement

This study was funded by Applied Basic Research Project (Agricultural) Suzhou Science and Technology Planning Programme (SNG2020061), Singapore Ministry of Education Academic Research Fund Tier 1 (R-160- 000-A40-114) and an industry grant from Shanghai ProfLeader Biotech Co., Ltd (R-160-000-A21-597).

Appendix A. Supplementary material

Supplementary data to this article can be found online at https://doi.org/10.1016/j.foodres.2022.111241.

References

Alteri, C. J., & Mobley, H. L. (2012). Escherichia coli physiology and metabolism dictates adaptation to diverse host microenvironments. *Current Opinion in Microbiology, 15*, 3–9.

Arunima, A., Swain, S. K., Patra, S. D., Das, S., Mohakud, N. K., Misra, N., & Suar, M. (2020). Role of OB-fold protein ydei in stress response and virulence of *Salmonella enterica* serovar enteritidis. *Journal of Bacteriology, 203*, e00237–20.

Arunima, A., Swain, S. K., Ray, S., Prusty, B. K., & Suar, M. (2020). RpoS-regulated SEN1538 gene promotes resistance to stress and influences *Salmonella enterica* serovar Enteritidis virulence. *Virulence, 11*, 295–314.

Bagamboula, C., Uyttendaele, M., & Debevere, J. (2004). Inhibitory effect of thyme and basil essential oils, carvacrol, thymol, estragol, linalool and p-cymene towards *Shigella sonnei* and *S. flexneri. Food Microbiology, 21*, 33–42.

Belenky, P., Jonathan, D. Y., Porter, C. B., Cohen, N. R., Lobritz, M. A., Ferrante, T., Jain, S., Korry, B. J., Schwarz, E. G., & Walker, G. C. (2015). Bactericidal antibiotics induce toxic metabolic perturbations that lead to cellular damage. *Cell Reports, 13*, 968–980.

Boskovic, M., Djordjevic, J., Ivanovic, J., Janjic, J., Zdravkovic, N., Glisic, M., Glamoclija, N., Baltic, B., Djordjevic, V., & Baltic, M. (2017). Inhibition of *Salmonella* by thyme essential oil and its effect on microbiological and sensory properties of minced pork meat packaged under vacuum and modified atmosphere. *International Journal of Food Microbiology, 258*, 58–67.

Bullwinkle, T. J., & Ibba, M. (2016). Translation quality control is critical for bacterial responses to amino acid stress. *Proceedings of the National Academy of Sciences, 113*, 2252–2257.

Chen, L., Zhang, H., Liu, Q., Pang, X., Zhao, X., & Yang, H. (2019). Sanitising efficacy of lactic acid combined with low-concentration sodium hypochlorite on *Listeria innocua* in organic broccoli sprouts. *International Journal of Food Microbiology, 295*, 41–48.

Chen, L., Zhao, X., Wu, J. E., Liu, Q., Pang, X., & Yang, H. (2020). Metabolic characterisation of eight *Escherichia coli* strains including“ Big Six” and acidic responses of selected strains revealed by NMR spectroscopy. *Food Microbiology, 88*, 103399.

Chin, K. C. J., Taylor, T. D., Hebrard, M., Anbalagan, K., Dashti, M. G., & Phua, K. K. (2017). Transcriptomic study of *Salmonella enterica* subspecies enterica serovar Typhi biofilm. *BMC Genomics, 18*, 1–9.

Chueca, B., Berdejo, D., Gomes-Neto, N. J., Pagán, R., & García-Gonzalo, D. (2016). Emergence of hyper-resistant *Escherichia coli* MG1655 derivative strains after applying sub-inhibitory doses of individual constituents of essential oils. *Frontiers in Microbiology, 7*, 273.

da Silva, L. I., Gomes-Neto, N. J., Magnani, M., & de Souza, E. L. (2015). Assessment of tolerance induction by *Origanum vulgare* L. essential oil or carvacrol in *Pseudomonas aeruginosa* cultivated in a meat-based broth and in a meat model. *Food Science and Technology International, 21*, 571–580.

Di Pasqua, R., Mauriello, G., Mamone, G., & Ercolini, D. (2013). Expression of DnaK, HtpG, GroEL and Tf chaperones and the corresponding encoding genes during growth of *Salmonella* Thompson in presence of thymol alone or in combination with salt and cold stress. *Food Research International, 52*, 153–159.

Djoko, K. Y., Phan, M.-D., Peters, K. M., Walker, M. J., Schembri, M. A., & McEwan, A. G. (2017). Interplay between tolerance mechanisms to copper and acid stress in *Escherichia coli. Proceedings of the National Academy of Sciences, 114*, 6818–6823.

Dong, R., Qin, X., He, S., Zhou, X., Cui, Y., Shi, C., He, Y., & Shi, X. (2021). DsrA confers resistance to oxidative stress in *Salmonella enterica* serovar Typhimurium. *Food Control, 121*, 107571.

Dubois-Brissonnet, F., Naïtali, M., Mafu, A. A., & Briandet, R. (2011). Induction of fatty acid composition modifications and tolerance to biocides in *Salmonella enterica* serovar Typhimurium by plant-derived terpenes. *Applied and Environmental Microbiology, 77*, 906–910.

Edrees, A., Abdelhamed, H., Nho, S. W., Park, S., Karsi, A., Austin, F. W., Essa, M., Pechan, T., & Lawrence, M. L. (2018). Construction and evaluation of type III secretion system mutants of the catfish pathogen *Edwardsiella piscicida. Journal of Fish Diseases, 41*, 805–816.

Fraňková, A., Marounek, M., Mozrová, V., Weber, J., Klouček, P., & Lukešová, D. (2014). Antibacterial activities of plant-derived compounds and essential oils toward *Cronobacter sakazakii* and *Cronobacter malonaticus. Foodborne Pathogens and Disease, 11*, 795–797.

Garai, P., Chandra, K., & Chakravortty, D. (2017). Bacterial peptide transporters: Messengers of nutrition to virulence. *Virulence, 8*, 297–309.

Giotis, E. S., McDowell, D. A., Blair, I. S., & Wilkinson, B. J. (2007). Role of branched-chain fatty acids in pH stress tolerance in *Listeria monocytogenes. Applied and Environmental Microbiology, 73*, 997–1001.

Grossoehme, N., Kehl-Fie, T. E., Ma, Z., Adams, K. W., Cowart, D. M., Scott, R. A., Skaar, E. P., & Giedroc, D. P. (2011). Control of copper resistance and inorganic sulfur metabolism by paralogous regulators in *Staphylococcus aureus*. *Journal of Biological Chemistry, 286*, 13522–13531.

Guo, J., Yang, R., Gong, Y., Hu, K., Hu, Y., & Song, F. (2021). Optimization and evaluation of the ultrasound-enhanced subcritical water extraction of cinnamon bark oil. *LWT-Food Science and Technology, 147*, 111673.

György, É., Laslo, É., Kuzman, I. H., & Dezső, A. C. (2020). The effect of essential oils and their combinations on bacteria from the surface of fresh vegetables. *Food Science & Nutrition, 8*, 5601–5611.

Hale, C. A., Shiomi, D., Liu, B., Bernhardt, T. G., Margolin, W., Niki, H., & de Boer, P. A. (2011). Identification of *Escherichia coli* ZapC (YcbW) as a component of the division apparatus that binds and bundles FtsZ polymers. *Journal of Bacteriology, 193*, 1393–1404.

Höferl, M., Buchbauer, G., Jirovetz, L., Schmidt, E., Stoyanova, A., Denkova, Z., Slavchev, A., & Geissler, M. (2009). Correlation of antimicrobial activities of various essential oils and their main aromatic volatile constituents. *Journal of Essential Oil Research, 21*, 459–463.

Hyldgaard, M., Mygind, T., & Meyer, R. L. (2012). Essential oils in food preservation: Mode of action, synergies, and interactions with food matrix components. *Frontiers in Microbiology, 3*, 12.

Jarrell, K. F., & Albers, S. V. (2012). The archaellum: An old motility structure with a new name. *Trends in Microbiology, 20*, 307–312.

Jarvis, N. A., O'Bryan, C. A., Dawoud, T. M., Park, S. H., Kwon, Y. M., Crandall, P. G., & Ricke, S. C. (2016). An overview of *Salmonella* thermal destruction during food processing and preparation. *Food Control, 68*, 280–290.

Khoo, C. H., Sim, J. H., Salleh, N. A., & Cheah, Y. K. (2015). Pathogenicity and phenotypic analysis of sop B, sop D and pip D virulence factors in *Salmonella enterica* serovar typhimurium and *Salmonella enterica* serovar Agona. *Antonie Van Leeuwenhoek, 107*, 23–37.

King, T., Lucchini, S., Hinton, J. C., & Gobius, K. (2010). Transcriptomic analysis of Escherichia coli O157:H7 and K-12 cultures exposed to inorganic and organic acids in stationary phase reveals acidulant-and strain-specific acid tolerance responses. *Applied and Environmental Microbiology, 76*, 6514–6528.

Kovács, J. K., Felső, P., Makszin, L., Pápai, Z., Horváth, G., Ábrahám, H., Palkovics, T., Böszörményi, A., Emődy, L., & Schneider, G. (2016). Antimicrobial and virulence-modulating effects of clove essential oil on the foodborne pathogen *Campylobacter jejuni. Applied and Environmental Microbiology, 82*, 6158–6166.

Lima, T. B., Pinto, M. F. S., Ribeiro, S. M., de Lima, L. A., Viana, J. C., Júnior, N. G., de Souza, Cândido E., Dias, S. C., & Franco, O. L. (2013). Bacterial resistance mechanism: What proteomics can elucidate. *The FASEB Journal, 27*, 1291–1303.

Liu, Q., Chen, L., Laserna, A. K. C., He, Y., Feng, X., & Yang, H. (2020). Synergistic action of electrolyzed water and mild heat for enhanced microbial inactivation of *Escherichia coli* O157:H7 revealed by metabolomics analysis. *Food Control, 110*, 107026.

Liu, Q., Je, W.u., Lim, Z. Y., Aggarwal, A., Yang, H., & Wang, S. (2017). Evaluation of the metabolic response of *Escherichia coli* to electrolysed water by ^{1}H NMR spectroscopy. *LWT-Food Science and Technology, 79*, 428–436.

Lu, M., Symersky, J., Radchenko, M., Koide, A., Guo, Y., Nie, R., & Koide, S. (2013). Structures of a Na^{+}-coupled, substrate-bound MATE multidrug transporter. *Proceedings of the National Academy of Sciences, 110*, 2099–2104.

Lund, P., Tramonti, A., & De Biase, D. (2014). Coping with low pH: Molecular strategies in neutralophilic bacteria. *FEMS Microbiology Reviews, 38*, 1091–1125.

Mazzarrino, G., Paparella, A., Chaves-López, C., Faberi, A., Sergi, M., Sigismondi, C., Compagnone, D., & Serio, A. (2015). *Salmonella enterica* and *Listeria monocytogenes* inactivation dynamics after treatment with selected essential oils. *Food Control, 50*, 794–803.

Mitchell, A. M., & Silhavy, T. J. (2019). Envelope stress responses: Balancing damage repair and toxicity. *Nature Reviews Microbiology, 17*, 417–428.

Mühlig, A., Behr, J., Scherer, S., & Müller-Herbst, S. (2014). Stress response of *Salmonella enterica* serovar Typhimurium to acidified nitrite. *Applied and Environmental Microbiology, 80*, 6373–6382.

Nabavi, S. F., Di Lorenzo, A., Izadi, M., Sobarzo-Sánchez, E., Daglia, M., & Nabavi, S. M. (2015). Antibacterial effects of cinnamon: From farm to food, cosmetic and pharmaceutical industries. *Nutrients, 7*, 7729–7748.

Paudel, S. K., Bhargava, K., & Kotturi, H. (2019). Antimicrobial activity of cinnamon oil nanoemulsion against *Listeria monocytogenes* and *Salmonella* spp. on melons. *LWT-Food Science and Technology, 111*, 682–687.

Pei, R. S., Zhou, F., & Ji Bp, XuJ. (2009). Evaluation of combined antibacterial effects of eugenol, cinnamaldehyde, thymol, and carvacrol against *E. coli* with an improved method. *Journal of Food Science, 74*, M379–M383.

Ramond, E., Gesbert, G., Rigard, M., Dairou, J., Dupuis, M., Dubail, I., Meibom, K., Henry, T., Barel, M., & Charbit, A. (2014). Glutamate utilization couples oxidative stress defense and the tricarboxylic acid cycle in *Francisella phagosomal* escape. *PLOS Pathogens, 10*, e1003893.

Rowlett, V. W., Mallampalli, V. K., Karlstaedt, A., Dowhan, W., Taegtmeyer, H., Margolin, W., & Vitrac, H. (2017). Impact of membrane phospholipid alterations in *Escherichia coli* on cellular function and bacterial stress adaptation. *Journal of Bacteriology, 199*, e00849–16.

Sanders, C., Turkarslan, S., Lee, D. W., & Daldal, F. (2010). Cytochrome c biogenesis: The Ccm system. *Trends in Microbiology, 18*, 266–274.

Swamy, M. K., Akhtar, M. S., & Sinniah, U. R. (2016). Antimicrobial properties of plant essential oils against human pathogens and their mode of action: An updated review. *Evidence-Based Complementary and Alternative Medicine, 2016*, 3012462.

Tan, K. C., Ipcho, S. V., Trengove, R. D., Oliver, R. P., & Solomon, P. S. (2009). Assessing the impact of transcriptomics, proteomics and metabolomics on fungal phytopathology. *Molecular Plant Pathology, 10*, 703–715.

Tanaka, K. J., Song, S., Mason, K., & Pinkett, H. W. (2018). Selective substrate uptake: the role of ATP-binding cassette (ABC) importers in pathogenesis. *Biochimica et Biophysica Acta (BBA)-Biomembranes, 1860*, 868–877.

Teoh, S. T., Putri, S., Mukai, Y., Bamba, T., & Fukusaki, E. (2015). A metabolomics-based strategy for identification of gene targets for phenotype improvement and its application to 1-butanol tolerance in *Saccharomyces cerevisiae*. *Biotechnology for Biofuels, 8*, 1–14.

Tsai, W. C., Zhuang, Z. J., Lin, C. Y., & Chen, W. J. (2016). Novel antimicrobial peptides with promising activity against multidrug resistant *Salmonella enterica* serovar Choleraesuis and its stress response mechanism. *Journal of Applied Microbiology, 121*, 952–965.

Visvalingam, J., Hernandez-Doria, J. D., & Holley, R. A. (2013). Examination of the genome-wide transcriptional response of *Escherichia coli* O157:H7 to cinnamaldehyde exposure. *Applied and Environmental Microbiology, 79*, 942–950.

Vong, W. C., Hua, X. Y., & Liu, S. Q. (2018). Solid-state fermentation with *Rhizopus oligosporus* and *Yarrowia lipolytica* improved nutritional and flavour properties of okara. *LWT-Food Science and Technology, 90*, 316–322.

Walter, W., Sánchez-Cabo, F., & Ricote, M. (2015). GOplot: An R package for visually combining expression data with functional analysis. *Bioinformatics, 31*, 2912–2914.

Wang, S., Phillippy, A. M., Deng, K., Rui, X., Li, Z., Tortorello, M. L., & Zhang, W. (2010). Transcriptomic responses of *Salmonella enterica* serovars Enteritidis and Typhimurium to chlorine-based oxidative stress. *Applied and Environmental Microbiology, 76*, 5013–5024.

Wesche, A. M., Gurtler, J. B., Marks, B. P., & Ryser, E. T. (2009). Stress, sublethal injury, resuscitation, and virulence of bacterial foodborne pathogens. *Journal of Food Protection, 72*, 1121–1138.

Yu, Y., Li, Z., Cao, G., Huang, S., & Yang, H. (2019). Bamboo leaf flavonoids extracts alleviate oxidative stress in HepG2 cells via naturally modulating reactive oxygen species production and Nrf2-mediated antioxidant defense responses. *Journal of Food Science, 84*, 1609–1620.

Yuan, W., Seng, Z. J., Kohli, G. S., Yang, L., & Yuk, H. G. (2018). Stress resistance development and genome-wide transcriptional response of *Escherichia coli* O157: H7 adapted to sublethal thymol, carvacrol, and trans-cinnamaldehyde. *Applied and Environmental Microbiology, 84*, e01616–18.

Zhang, X. S., García-Contreras, R., & Wood, T. K. (2007). YcfR (BhsA) influences *Escherichia coli* biofilm formation through stress response and surface hydrophobicity. *Journal of Bacteriology, 189*, 3051–3062.

Zhang, Y., Liu, X., Wang, Y., Jiang, P., & Quek, S. (2016). Antibacterial activity and mechanism of cinnamon essential oil against *Escherichia coli* and *Staphylococcus aureus*. *Food Control, 59*, 282–289.

Zhao, L., Zhao, X., Je, W.u., Lou, X., & Yang, H. (2019). Comparison of metabolic response between the planktonic and air-dried *Escherichia coli* to electrolysed water combined with ultrasound by ^{1}H NMR spectroscopy. *Food Research International, 125*, 108607.

Zhao, X., Chen, L., Je, W.u., He, Y., & Yang, H. (2020). Elucidating antimicrobial mechanism of nisin and grape seed extract against *Listeria monocytogenes* in broth and on shrimp through NMR-based metabolomics approach. *International Journal of Food Microbiology, 319*, 108494.

Zhao, X., Chen, L., Zhao, L., He, Y., & Yang, H. (2020). Antimicrobial kinetics of nisin and grape seed extract against inoculated *Listeria monocytogenes* on cooked shrimps: Survival and residual effects. *Food Control, 115*, 107278.